



OPEN ACCESS

EDITED BY

Stanislaw Mazur,
Polish Academy of Sciences, Poland

REVIEWED BY

Emanuele Lodolo,
National Institute of Oceanography and
Experimental Geophysics, Italy
Andrzej Konon,
University of Warsaw, Poland

*CORRESPONDENCE

Xijie Feng,
✉ 593721146@qq.com

RECEIVED 20 December 2022

ACCEPTED 10 April 2023

PUBLISHED 17 April 2023

CITATION

Li W and Feng X (2023), Discovery of the Qinghe fault, the inner part of the Weihe graben, central China, and its geological significance.
Front. Earth Sci. 11:1127897.
doi: 10.3389/feart.2023.1127897

COPYRIGHT

© 2023 Li and Feng. This is an open-access article distributed under the terms of the [Creative Commons Attribution License \(CC BY\)](https://creativecommons.org/licenses/by/4.0/). The use, distribution or reproduction in other forums is permitted, provided the original author(s) and the copyright owner(s) are credited and that the original publication in this journal is cited, in accordance with accepted academic practice. No use, distribution or reproduction is permitted which does not comply with these terms.

Discovery of the Qinghe fault, the inner part of the Weihe graben, central China, and its geological significance

Wei Li^{1,2} and Xijie Feng^{3*}

¹Institute of Geology, China Earthquake Administration, Beijing, China, ²The Second Monitoring and Application Center, China Earthquake Administration, Xi'an, China, ³Shaanxi Earthquake Agency, Xi'an, China

The Weihe graben is an active Cenozoic continental rift with frequent seismic activity. The previous work focused on the graben boundary faults, but less work has been conducted on the faults in the internal graben. The Weihe basin is an economically developed and densely populated area. Therefore, identifying these potential risks is significant for the evaluation of regional seismic hazards and to understand the evolution of continental rifts. Prior work used oil exploration methods to document a fault (we named it "Qinghe fault") in the Qinghe river area of Sanyuan County, north of Xi'an. But the shallow structure and activity was not clear. Therefore, we carried out shallow seismic detection and borehole exploration, as well as a geological survey in the area. Based on seismic reflection profile and boreholes, the Qinghe fault is the main fault and with other secondary faults, together they constitute a typical Y-shaped structure, with a fracture zone width ~4 km. Combined with the field survey, we provide evidence that the Qinghe fault is a Holocene active fault and capable of earthquakes of magnitude 5.2–5.5. The discovery of the Qinghe fault shows that the Weihe rift is active, and the faults inside the rift play an important role in tectonic deformation.

KEYWORDS

Weihe graben, Qinghe fault, seismic reflection profile, boreholes, seismic assessment

1 Introduction

The Cenozoic graben systems around the tectonically stable Ordos block, central China (Figure 1A) have been considered ideal places for investigating the development and evolution of continental rifts, as well as slip behaviors of active normal faults associated with high historical seismicity (Deng et al., 1984; Wesnousky et al., 1984; SSB, 1988; Zhang et al., 1995; 1998). Although large-magnitude, intracontinental earthquakes generated by normal faulting are uncommon (McCalpin, 2009), the Weihe graben south of the Ordos block is characterized by large earthquakes, where three historical earthquakes of $M \geq 7$ occurred in the past 2,800 yrs (Figure 1B).

The Weihe basin is an important part of the Fenwei active faulted depression, in which deposition begun in the Eocene. Under the influence of the uplift of the Tibetan Plateau, the NW-SE horizontal extension and left-lateral shear occurred in the late Cenozoic and continued until the late Quaternary (Molnar and Tapponnier, 1975; Zhang et al., 1998), which resulted in the development of active faults and frequent strong earthquakes in this area. Although the magnitude estimates mainly rely on seismic-induced damages and hence

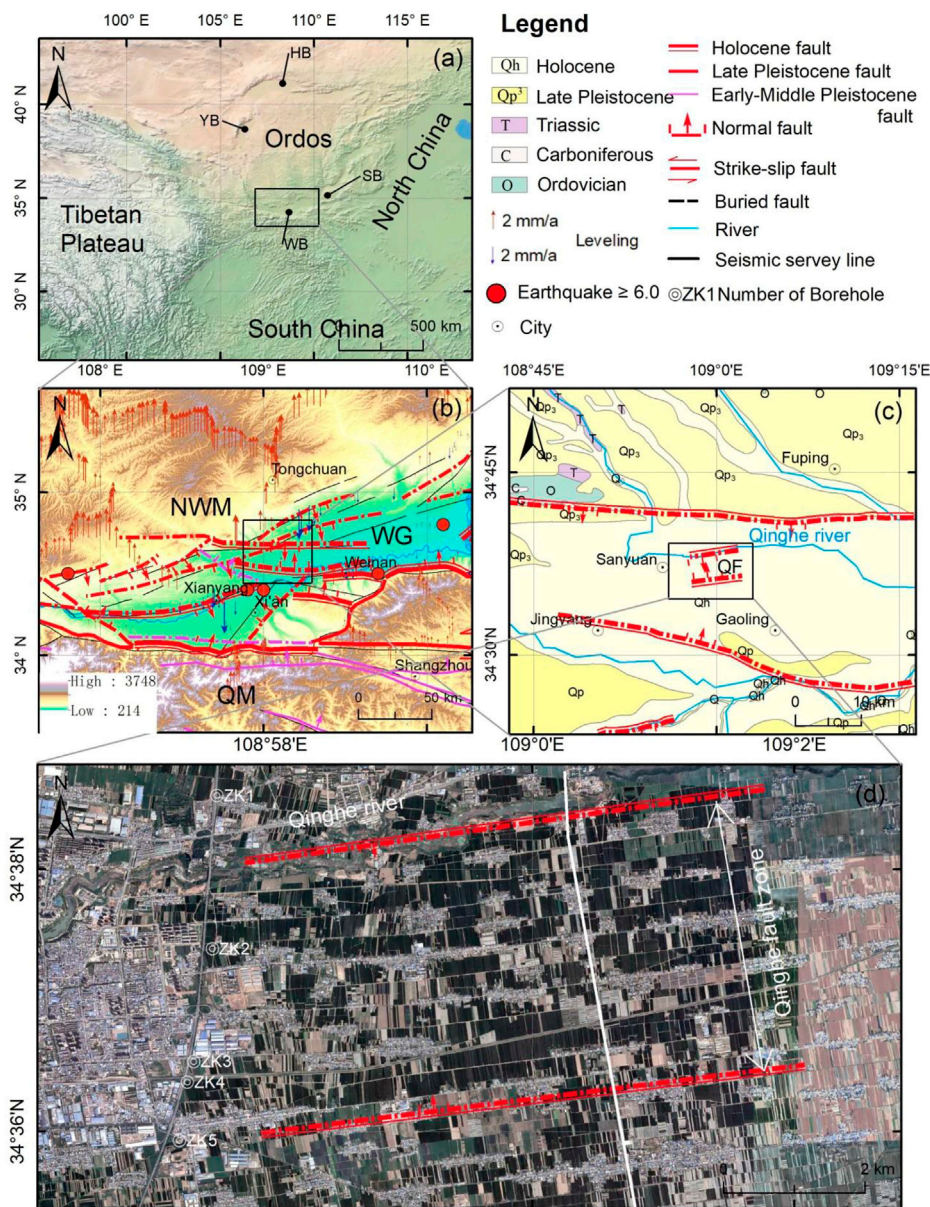


FIGURE 1

(A) Regional topographic map. The black rectangle represents the location of the Weihe graben Figure1B. WB: Weihe basin; YB: Yinchuan basin; SB: Shanxi basin; HB: Hetao basin. (B) Active tectonics of the Weihe graben, showing the distribution of the major active faults and large historical earthquakes of the graben systems. The vertical arrow represents the vertical leveling velocity field relative to ITRF 2008 (Data from Hao et al., 2016). WG: Weihe graben; QM: Qinling Mountains; NWM: North Weibe Mountains. (C) Geological map of the study area. QF, Qinghe fault. (D) Location of seismic detection zone, showing seismic reflection profile, boreholes, and interpreted faults. The solid white line represents the shallow seismic line. The base image is the GoogleEarth image.

might be overestimated (Middleton et al., 2016; Xu et al., 2018), a future earthquake is likely to be destructive as the neighboring megacity of Xi'an now has a population of 10 million people.

In the past few years, research on the boundary faults with a capacity of large earthquakes around the Weihe graben has gradually increased (Zhang, 1991; Rao et al., 2014; Rao et al., 2015; Cheng et al., 2018; He et al., 2020; Yang et al., 2021). However, because of rapid subsidence in the interior of the Weihe basin, the late Quaternary sediments are well developed, and the landforms have been severely eroded and transformed. Therefore, research on active faults of the

internal graben is limited to small sections of the faults (Shi et al., 2007; Feng et al., 2008; Li et al., 2008; Shi et al., 2009; Ma et al., 2019). In addition, due to the uncertainty of the historical earthquake records on active faults in the interior of the Weihe graben, the tectonic activity and seismic risk here has been highly underestimated. More importantly, there may still be other buried active faults with strong earthquake potential that have not yet been detected in the basin. Exploring and identifying these potential hazards is of great value for understanding the evolution and deformation patterns of continental rifts, and to assess the risk of earthquakes.

According to oil exploration data in the Weihe basin in the 1960s, there is a NE- EW trending fault in the Qinghe river area of Sanyuan County (Figure 1C), called the “Qinghe fault” (Abbreviated as “QF”). In the seismic reflection structure map of the middle and deep layers of the Weihe basin, the QF extends eastward along the Qinghe river, and has an east-west strike, inclined to the south, with a dip angle of 70° and a length of about 34 km. The offsets of the shallow reflector, middle reflector and deep reflector are 50–200 m, 650–800 m and more than 800 m, respectively (The third census exploration team of the State General Administration of Geology, 1977).

In this study, we conducted shallow seismic exploration and borehole surveys on the QF in order to better reveal the structure and characteristics of the QF and understand its activity. In combination with field observations, rupture characteristics and seismic risk for the QF are examined. The results presented in this study will be helpful in better understanding characteristics of active normal faulting in continental rifts, and deformation and evolution models of continental rifts.

2 Tectonic setting

The Weihe basin is located in the central part of Shaanxi Province, between the Qinling Mountains and the North Weibei Mountains. It is about 300 km long with a horn shape that is narrow in the west and wide in the east, with an area of about 49,400 km² (Figure 1). The average elevation is 323–800 m. The Weihe basin has a warm temperate semi-humid climate, with an average annual temperature of 12–13.6°C and an annual precipitation of 550–660 mm.

During the Yanshan orogeny, the Ordos block showed intermittent uplift and subsidence movements, while strong tectonic activity occurred on its periphery. In the Hetao and Weihe basins, a near east-west trending compressional tectonic belt has formed, while a NE-NNE trending compressional tectonic belt has formed in the Shanxi and Yinchuan basins. The basic tectonics during the Mesozoic, especially the Yanshan orogen, laid the foundation for the Cenozoic geological evolution of the area. During the Cenozoic era, the most outstanding event of the southwestern margin and adjacent areas of Ordos were the formation of a series of extensional faulted basins on its periphery and the formation of a thrust fault zone on its southwestern margin. During this period, the Ordos region was mainly controlled and influenced by two major dynamic systems: first, the Indian and Eurasian plates collided with each other, leading to the rise of the Tibetan Plateau and eastward extrusion; second, the Pacific plate was being subducting westward, resulting in the formation of the above-mentioned structural systems. According to the sediment distribution of the Ordos block and the developmental characteristics of the faulted zones, the tectonic activity of the area can be roughly divided into three main stages as follows: (1) the Weihe basin, the Yinchuan basin, and the Jilantai basin, which began to develop in the Eocene and basically formed at the end of the Oligocene. At this time, the southwestern margin of the block was compressed, forming the curved structure boundary in the Baoji-Liupanshan area; (2) at the end of the Miocene, the Ordos block continued to rise and the peripheral faulted zones continued to

develop. In addition, the Weihe faulted zone extended eastward into Shanxi, forming the Yuncheng basin; (3) at the end of the Pliocene, the Shanxi faulted zone was basically forming. At the same time, intense compression due to the NE-wards expansion of the Tibetan Plateau occurred on the southwestern margin of Ordos, and the arc-shaped deformation belt was built up (SSB, 1988; Deng et al., 1999; Deng et al., 2003; Zhang et al., 2006; Zhao et al., 2017; Su et al., 2021).

Since the Paleogene, under the influence of the Himalayan orogeny, Mesozoic uplift in the area ceased, with large-scale rift extension and overall subsidence. Due to the activity of the faults controlling the southern margin of the Weihe basin, the faults inside the basin were activated. Several secondary faulted blocks formed in the basin, with significant differences in activity (SSB, 1988). The tectonic geomorphology of the Weihe basin includes adjacent faulted-block mountains outside the basin, gentle loess Tableland, alluvial fans and river terraces in the basin, etc. From the Qinling Mountains and the Beishan Mountains on the southern margin of Ordos to the center of the basin, is a stepped multi-layered landscape. Many types of landforms and complex structures exist inside the basin (Figure 1B).

The thickness of the Cenozoic sediments in Weihe basin is between 2000 and 7,000 m. Affected by the tectonic tilt, the thickness of the sediments gradually decreases to the north. The Quaternary sediments in the Weihe basin are up to 1,200 m thick, and the average deposition rate is 465 m/Ma, much higher than the Tertiary deposition rate of 80 m/Ma, indicating the rapid uplift of the Qinling Mountains and the accelerated subsidence of the Weihe basin during the Quaternary (Sun, 2005; Sun and Xu, 2007; Rao et al., 2014).

The sedimentary types of the Weihe basin is also obviously controlled by tectonic processes. In its southern part, Sanmen lake formed due to the strong depression of the Qinling Mountains. The age of the fluvial and lacustrine strata is from the late Pliocene to the early Pleistocene (Han et al., 1997), overlaid by the middle Pleistocene to Holocene Loess-Paleosol Sequence. In its northern part, the lacustrine facies strata are lacking, replaced by Tertiary Tritoe horse red clay, and overlaid by the Quaternary loess. All Tertiary and Quaternary strata are not folded and deformed, indicating that the tectonic movement since the late Cenozoic is characterized by vertical movement (Sun and Xu, 2007).

Based on precise regional leveling data, the Weihe graben is subsiding at rates of 4–6 mm/a with respect to the central Ordos block (Hao et al., 2016; Figure 1B). GPS stations in the study area are too few to accurately characterize the movements of individual fault (Qu et al., 2014). The GPS results of Zhao et al. (2017) indicate no obvious deformation in Weihe rift. A dense GPS velocity field coverage for the Ordos block and the surrounding region suggests that the Weihe graben experienced slight extensional deformation but no detectable shear deformation (Hao et al., 2021).

3 Methods and results

3.1 Seismic reflection profile

In order to determine the specific location, geometric structure, tendency, width and burial depth of the QF, we acquired an approximately N-S shallow seismic line ~6 km east of Sanyuan

TABLE 1 Parameters and requirements of the shallow seismic survey.

No.	Parameters	Values and methods
1	Length of survey line	~ 6 km
2	Vibration source stimulation method	Vibration control vehicle stimulation
3	Receiving method	bilateral asymmetric reception
4	Distance between tracks and distance between shots	2–4 m; 8–20 m
5	Coverage	≥ 20
6	Effective receiving channels	≥ 120
7	Effective detection depth	100–300 m
8	Depth error	≤ 8%
9	Horizontal positioning error of fault	≤ 15 m



County (Figure 1D). The details of the shallow seismic survey are listed in Table 1.

The shallow seismic exploration data were processed using GeoEast software. The main processing module flow of the reflection data included: (1) elevation static correction; (2) amplitude compensation; (3) deconvolution; (4) velocity analysis and residual static corrections; (5) post-stack noise reduction and an offset test.

The survey line direction is nearly perpendicular to the QF. The survey line was laid along a road, where surface stimulation and geophone receiving conditions are good. The seismic detection zone is flat and located in an alluvial plain. Good Holocene strata are

exposed on both banks of the Qinghe river. As shown in Figure 2A, the horizontal bedding has typical alluvial-colluvial characteristics, providing a good marker strata (Figure 2B). The sediments in the seismic detection zone are relatively thick, with well-developed sedimentary facies, which correspond to abundant acoustic impedance contrasts.

Figure 3 illustrates our seismic profile after processing. The time profile shows that the signal-to-noise ratio in the profile is high, and reflections are well developed, which is helpful for tracking the stratigraphic horizons. A total of five reflections (T1, T2, T3, T4, T5 in Figure 3) are examined, all of which are within the Quaternary sediments (Figure 3). From the profile, the strata as a whole are slightly inclined southward. The closer to the fault, the dip angle gradually increases, accompanied by drags and folds (Figure 3).

The exploration results show (Figure 3) that a large-scale main fault dipping to the south has developed along the Qinghe river. On the south side of the main fault, five secondary faults dip to the north (f1, f2, f3, f4, f5 in Figure 3), together constituting a small composite graben, with a width of the fracture zone in the plane of the section of about 4 km. The dip of the faults is about 70°–80° in the upper section of the profile, and gradually decreases.

3.2 Boreholes

In order to verify the geophysical interpretations, and document activity on the QF, five boreholes were drilled on the fault zone, roughly perpendicular to the fault and parallel to the seismic profile. The location of the boreholes is shown in Figure 1D. The details of the boreholes are found in Table 2.

The first paleosol layer (S_1) in the boreholes is well-developed, continuous horizontally, and has characteristics different from the upper and lower strata. In addition to the bright reddish-brown color, the S_1 has a well-developed soil architecture (Figure 4), which also provides a nice seismic marker.

Extensive research has been done on the ages of the regional S_1 paleosol layers (Table 3; Sun and Xu, 2007; Lei and Yue, 1997; Lei et al., 1992; Chen et al., 1999; Ding and Liu, 1989; Liu and Ding, 1990; Ma et al., 2019; Yang et al., 2021). Five levels of fluvial terraces are developed in the Weihe graben, and these terraces are

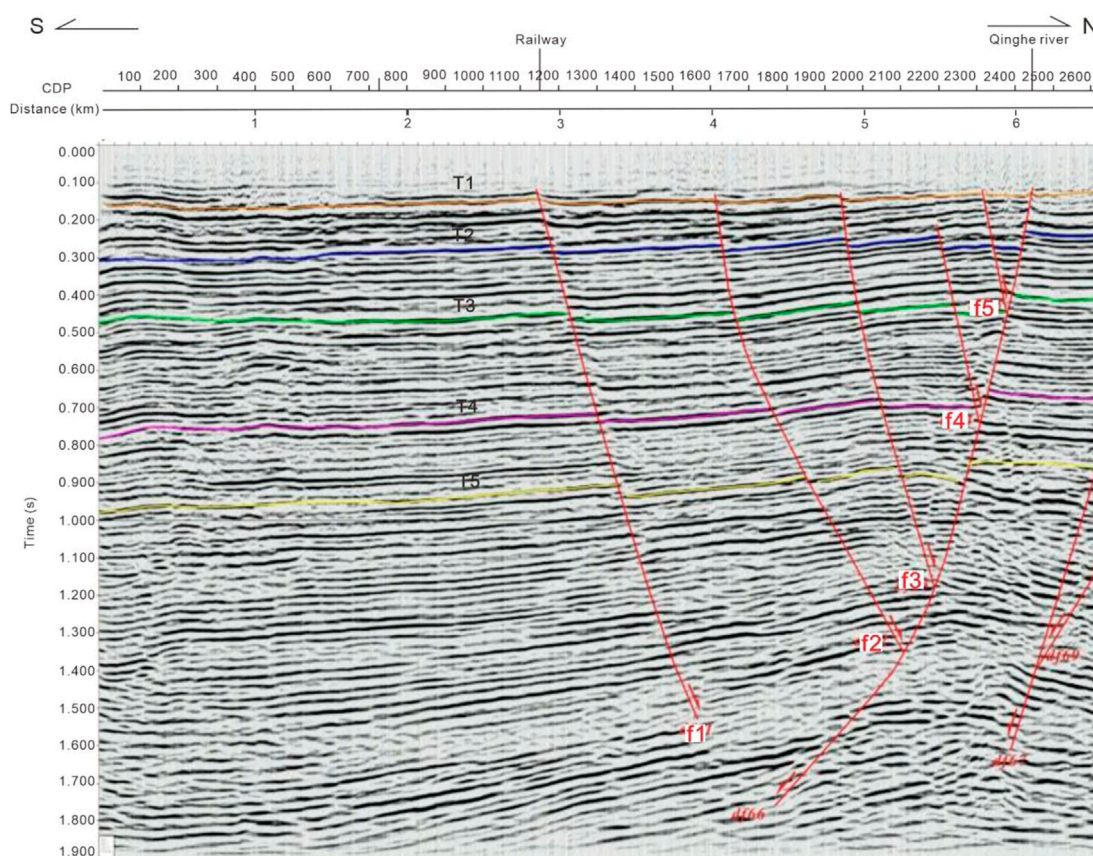


FIGURE 3 Interpretation of seismic survey line. The abscissa is the distance, and the ordinate is the time. T1, T2, T3, T4, T5 are reflections marked in different colors. f1, f2, f3, f4, f5 are interpreted secondary faults.

TABLE 2 The locations and depths of the boreholes.

No.	Longitude and latitude	Depth (m)	Elevation (m)
ZK1	108°57'35.7" 34°38'33.9"	69.2	387.1
ZK2	108°57'33.5" 34°37'23.7"	30.5	383.9
ZK3	108°57'25.0" 34°36'32.0"	72.0	380.8
ZK4	108°57'22.1" 34°36'22.5"	71.8	380.3
ZK5	108°57'18.5" 34°35'55.8"	30.0	379.0

composed of the riverbed facies at the bottom and the Quaternary aeolian sediments above. The loess layers at the bottom of the five terraces are L₃₃, L₁₅, L₉, L₆ and L₂. On the basis of magnetostratigraphy and climatic stratigraphy, the above-mentioned loess layers correspond to the deep-sea oxygen isotope stages 104, 36, 22, 16 and 6, respectively; the ages of the terraces are 2.60 Ma, 1.20 Ma, 0.90 Ma, 0.65 Ma, and 0.15 Ma, respectively (Sun and Xu, 2007). The geological environment of the study area belongs to the alluvial plain of the Weihe river, and the landform belongs to the T1 terrace. Thus, the S₁ paleosol of the T1 terrace, located in the upper part of the L₂ loess, close to

~0.15 Ma. Lei and Yue. (1997) concluded that the S₁ palaeosol formed in the late Pleistocene of the Guanzhong Basin in Shaanxi during the period of about 130–75 ka B.P. (the last interglacial period) was composed of four layers of paleosol and three layers of loess. The L₁ loess accumulated during the 75–10 ka B.P. period (last glacial period) can be divided into three layers of loess and two layers of weakly developed soil.

In order to visualize the location and activity of the fault in the study area, a profile of the borehole descriptions was made (Figure 5). As shown in Figure 5, the boreholes ZK4 and ZK5 in the southern area are 800 m apart, and the bottom elevations of the S₁ paleosol layers are 363.91 m and 362.67 m, respectively, leaving a difference of 1.3 m. While the ZK3 and ZK4 are only 300 m apart, the bottom elevations of the S₁ paleosol layers are 366.50 m and 363.91 m, respectively. An offset of 2.6 m thus exists between ZK3 and ZK4, consistent with a late Pleistocene fault displacing the S₁ (Figure 5).

Similarly, ZK2 and ZK3 in the middle part of the study area are 1,600 m apart, and the bottom elevation of the S₁ is 362.93 m and 366.50 m, respectively. The bottom elevation of the S₁ paleosol layer of the ZK2 on the northern side is 3.5 m lower. This implies a fault between ZK2 and ZK3, active since the late Pleistocene (Figure 5).

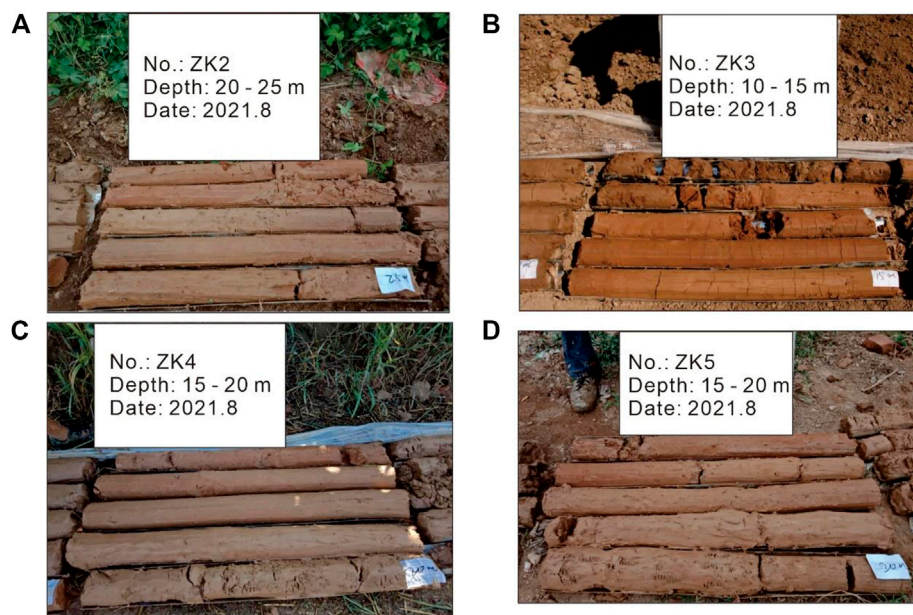


FIGURE 4
(A–D) Photographs of late Pleistocene paleosol strata (S_1) revealed by cores extracted from the boreholes. The contents inside the white panels denote the boreholes number, core depths and drilling dates, respectively.

TABLE 3 The ages of the regional S_1 paleosol layers.

Ages	Reference stratigraphy	Citation sources
0.13–0.18 Ma	Loess layer L_2 at the bottom of the T1 terrace of the Weihe river, overlaid by S_1	Sun and Xu. (2007)
0.075–0.13 Ma	Ages of the bottom and top of the S_1 , determined based on available dating data	Lei and Yue. (1997)
0.11–0.12 Ma	TL age of the first S_1 reddish-brown paleosol layer of T2 terrace of the Bahe river	Lei et al. (1992)
0.13 Ma	Age of the bottom of the S_1 paleosol of the T2 terrace in the Baoji section of the Weihe river	Chen et al. (1999)

3.3 Field observation and activity

A geological field investigation was carried out along the main fault and secondary faults interpreted from the shallow seismic profile. A large number of structural tensional fissures were found developed in Holocene strata (Figure 6), striking east-west. Most of these fissures are generally perpendicular to the ground surface or strata, and are filled with dark brown consolidated veins (Figures 6, 7), causing sharp contrast with the strata on both sides. The veins in the tectonic fissures can often be the silty and fine sand produced by the sand liquefaction accompanying the earthquake process. The scale of these fissures ranges from a few centimeters up to 10 cm to tens of centimeters. Where the vertical exposure is better, they can be seen to cut through Holocene strata (Figure 6A). The fissures formed by tectonic stress are called tectonic fissures. Since tectonic stress has a certain direction in a region, the distribution of various tectonic fissures formed by tectonic stress in nature is regular, and the arrangement direction is certain. In addition, tectonic fissures have good extension in both horizontal and vertical directions, mainly concentrated in and near the fault zone, and generally

parallel to the fault strike. The direction of cracks generated by non-tectonic stress (oil processes/internal deformation of unconsolidated materials) can be random or in multiple groups, and the distribution is relatively local. The tectonic fissures in the field are mainly located inside the Qinghe fault zone, outside the fault zone, these tectonic fissures are not observed. Therefore, we can be sure that these must be due to tectonic faulting.

In addition, we also observed signs of two phases of activity (Figure 7), indicating that the fault is quite active. The fissures formed by an early earthquake event (T1) were filled with veins, and the veins were subsequently consolidated; the fissures formed by a later earthquake event (T2) cut through and staggered the veins formed earlier (Figure 7). In some locations, the Holocene gray-black soil layer is vertically offset (Figure 8), demonstrating Holocene activity on the fault.

The Quaternary stratigraphy of this area was established by the early standard borehole detection data. The results show that the bottom of the Holocene is roughly 6–8 m, that of the late Pleistocene is roughly 78–104 m, and that of the middle Pleistocene is roughly 470–620 m (Table 4; Figure 9; The third census exploration team of the State General Administration of Geology, 1970s). In

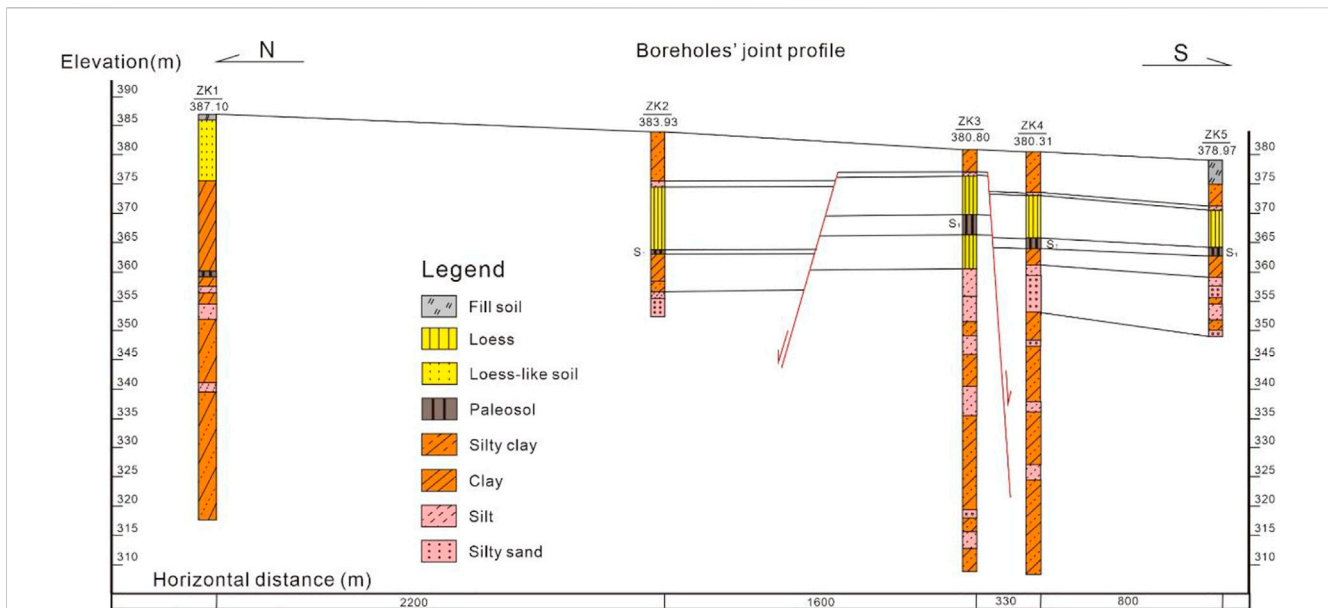


FIGURE 5 Drilling profile.

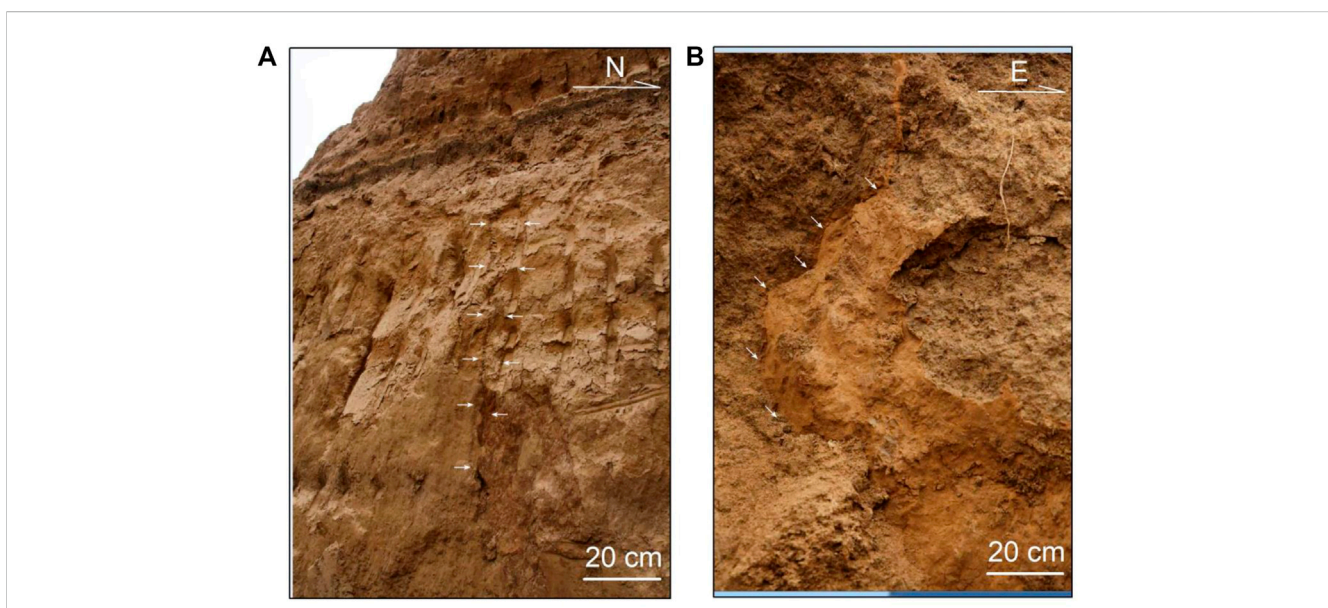


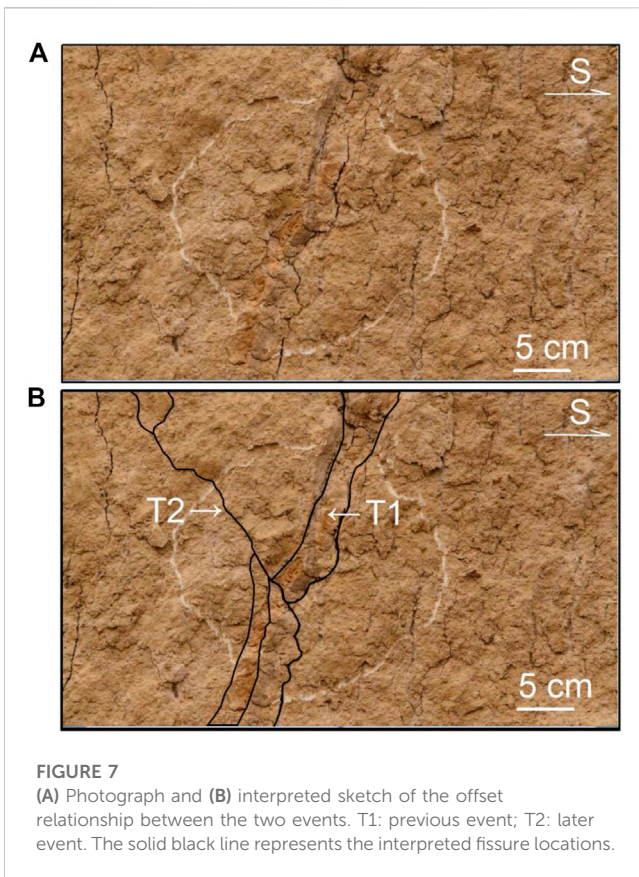
FIGURE 6 (A) and (B) Photograph of fissures developed in Holocene strata. Thin white arrows indicate the fissures.

addition, according to the 1:200,000 geological map of this area, the thickness of the alluvial deposits in the lower and upper Holocene are 1–5 m and 5–29 m respectively. The lower Holocene constitutes low terrace sediments, mainly composed of loess-like sandy clay, loam, and sand-gravel layer. The upper Holocene constitutes a modern riverbed, which is mainly composed of alluvial sand, gravel and a small amount of loam. The structural fissures and outcrops of displaced strata we observed in the field are all located on the surface, it is thus certain that the latest activity of the QF is the Holocene.

4 Discussion

4.1 Rupture characteristics and activity of the QF

Our seismic line is consistent with previous petroleum geophysical data (Figure 10; Xijie Feng, personal communication), with respect to the largest main fault situated in the Qinghe river area, parallel to the Qinghe river, which strikes



east-west. The difference between the two results is that the multiple secondary faults discovered this time on the south side of the main fault were not identified because the oil exploration target layer was beyond this group of secondary faults.

The rupture characteristics of the Qinghe fault could be manifested in two ways, and its geometry structure is instructive for study and comparison to the internal faults in other basins (Zhang, 1991; Shi et al., 2007; Feng et al., 2008; Lei et al., 2008; Li et al., 2008; Shi et al., 2009; Rao et al., 2014; Rao et al., 2015; Cheng et al., 2018; Ma et al., 2019; He et al., 2020; Yang et al., 2021). One is that the Qinghe fault zone is larger in scale. Many secondary reverse faults are the same size as the main fault, that together with the main fault, forms a “Y”-shaped composite graben (Figure 3). On the other hand, the width of the fault zone of the Qinghe fault reaches about 4 km in the plane of the section (Figure 10), which is rare on other faults in the basin. However, the deformation on both sides of the Qinghe fault is most controlled by the main fault.

Based on the above characteristics, we interpret the deformation in the area has concentrated on the main fault of the Qinghe fault zone, and the strain release is mainly borne by the main fault. The secondary faults absorb and accommodate the release of stress and strain in the interior of the fracture zone, dominated by post-seismic and inter-seismic deformation. The scale of the secondary faults limits the capacity to generate a large earthquake alone compared with the main fault. Such a wide fracture zone and complex structure might be attributed to the repeated dislocations caused by multiple earthquakes.

Although the Qinghe fault was discovered as early as the 1960s, its detailed shallow structure has once been ascertained in recent years. Due to the limited work on the activity of the fault, its seismic risk has not received much attention. Our detailed field surveys show that the Qinghe fault developed many structural fissures on the surface that cut Holocene strata (Figures 6, 8). These observations suggest the Qinghe fault is an active Holocene fault. Combined with the multi-stage fissures we have observed (Figure 7), the Qinghe fault appears to have been active since the late Pleistocene to

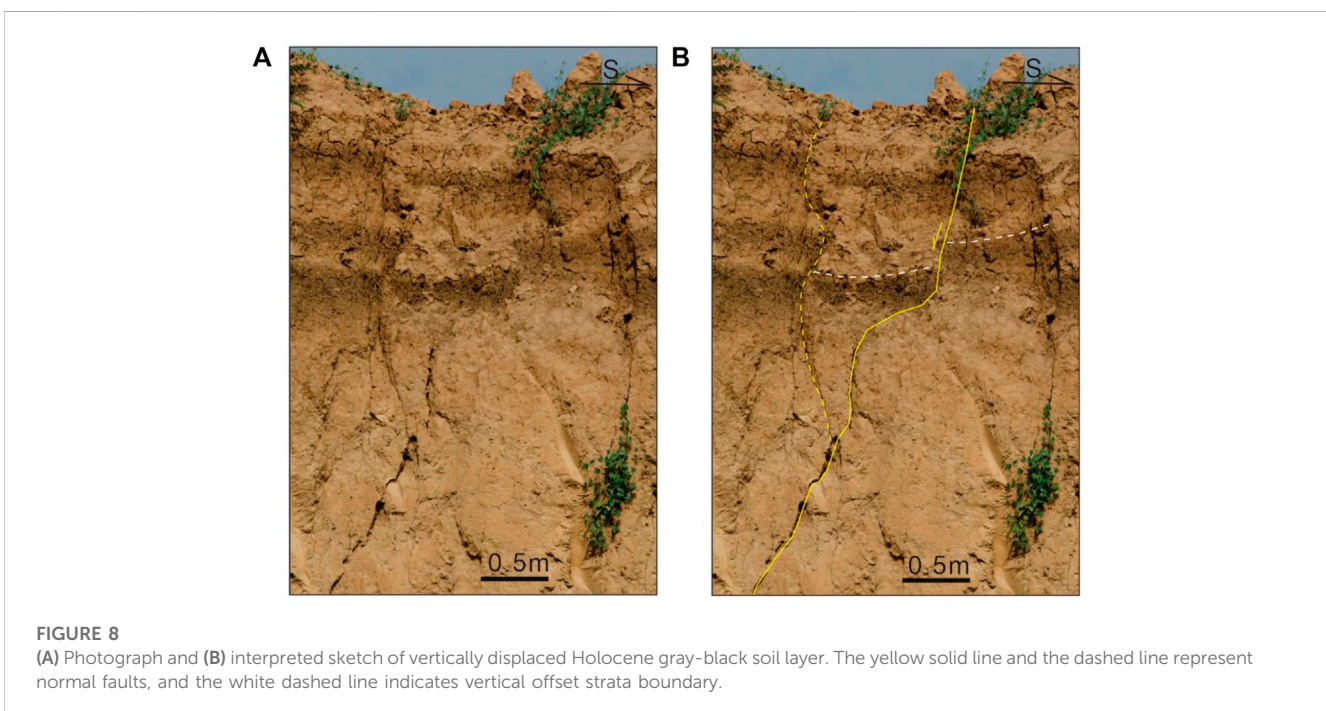


TABLE 4 Standard borehole detection and Quaternary stratigraphy in Weihe basin.

No.	Name	Location	Elevation	Depth	P ₂ sh	E	N ₁ g ¹	N ₂ yl ⁴	N ₂ yl ¹⁻³	Q ₁	Q ₂₋₄
1	S1	Jingyang	413.84	1,183.18				309.68	266	160.5	447.0
2	SW1	Gaoling	392.59	2,518.52			588.52	747.75	411.75	168.0	603.0
3	SW3	Sanyuan	424.4	2,669.92	74.42	495.7	641.3	530.5	288.0	150.0	490.0
4	SW7	Xian	364.63	2,745.18			560.18	879.5	513.75	310.5	481.25
5	SW16	Lintong	355.77	3,504.1			391.6	831.0	1,182.0	470.0	683.5
6	SW17	Yanliang	377.7	2,887.59			81.59	645.0	1,036.0	508.0	617.0

All the units are meters.

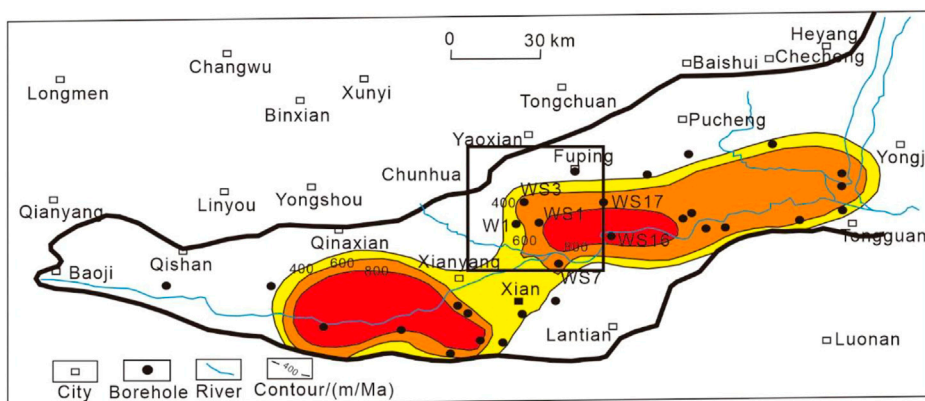


FIGURE 9

Standard borehole detection and Quaternary stratigraphy contour map in the Weihe basin. We have marked the abbreviations of six standard boreholes consistent with Table 4. The thick black solid line represents the basin boundary, and the black rectangle indicates the extent of the study area.

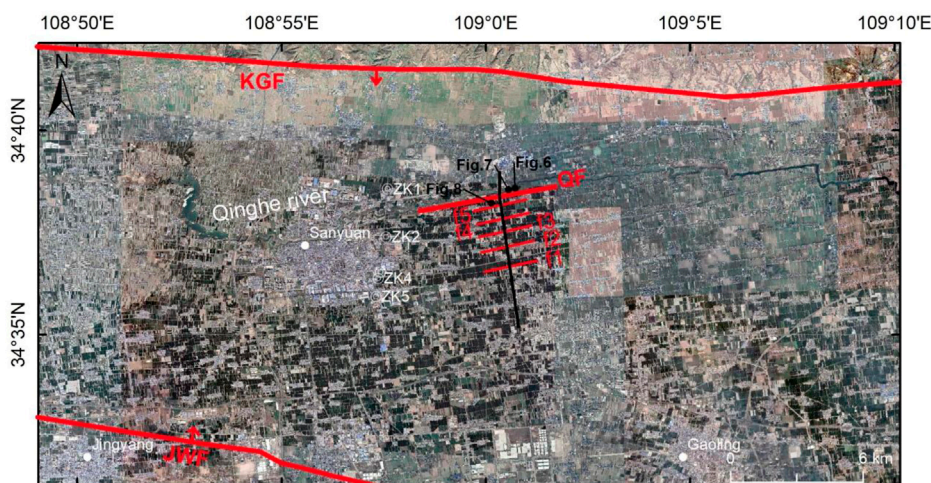


FIGURE 10

Morphostructural map of the study area. The red thick solid line represents the main faults, the red thin solid line represents the surface projection of the secondary faults interpreted in this work, black solid line represents the shallow seismic survey line. The white bicentric circles represent the boreholes, and the black dots indicate the field observation points in Figures 6–8. QF: Qinghe fault; KGF: Kouzhen-Guanshan fault; JWF: Jingyang-Weinan fault.

Holocene and may have the potential to generate moderate to strong earthquakes.

4.2 Seismic assessment and tectonic significance

As earthquake magnitude is well-known to be positively correlated with fault rupture features (Wells and Coppersmith, 1994), the evaluation of rupture characteristics of potentially seismogenic faults is important for seismic risk assessment. Some recent research shows that normal fault earthquakes have smaller upper limits to their magnitudes than thrusts, because their relatively steep dips produce intersections at the base of the seismogenic layer at smaller downdip widths than gently dipping thrust faults: for a given seismogenic thickness, a normal fault dip-slip rupture reaches the full limit of the seismogenic layer at a smaller distance than a thrust, thereby limiting the maximum size of the earthquake (Middleton et al., 2016; Xu et al., 2018). However, in order to limit the upper bound of the highest earthquake magnitude in the study area, we adopt a maximum deformation parameter as a criterion for the seismic fortification of engineering buildings. The width of the Qinghe fault zone is about 4 km, so we refer to this value as the subsurface rupture width. Utilizing the empirical relationship between the magnitude and subsurface rupture width of Wells and Coppersmith (1994), an earthquake magnitude of 5.2–5.5 could be a conservative estimate.

In addition to the strong ground motion caused by the earthquake, the liquefaction of sand is one of the common secondary disasters of large earthquakes, especially the plains or basins distributed in the Quaternary and close to the earthquake area, and these areas are often densely populated and built. Therefore, an in-depth understanding of the earthquake sand liquefaction phenomenon is an important part of disaster reduction and prevention (Liu-Zeng et al., 2017). Liquefaction of sand refers to the phenomenon in which water-saturated loose silty fine sand are suddenly destroyed under the vibration and become liquid. Due to the increase of pore water pressure and the decrease of effective stress, the sand changes from solid to liquid state. Sand liquefaction can occur on a large scale during earthquakes and cause serious damage. In China's 1966 Xingtai earthquake, 1975 Haicheng earthquake and 1976 Tangshan earthquake and other major earthquakes, the damage to some buildings was caused by the liquefaction of sand. The liquefaction of sand is also common in the active fault zone of the Weihe basin (Wang et al., 2018; Ma et al., 2019; Yang et al., 2021). Considering the developed loose late Quaternary sediments in the study area and a large number of fissures found in the field, a detailed investigation and study of the Qinghe fault and its fissures are important for preventing earthquake's secondary disasters. In addition, seismic-induced sand liquefaction is also an important means to study historical earthquakes and paleo-earthquakes, and the results are of great significance for evaluating the earthquake hazards in the region.

Next, we briefly discuss the tectonic significance of the Qinghe fault from the perspective of continental rifts. The Weihe rift and other rifts (Shanxi rift system, Yinchuan rift, Jilantai rift, Hetao rift) around the Ordos block differ significantly in tectonic activity (Deng et al., 1984; Deng and Liao, 1996; Lei et al., 2008; Middleton et al., 2017; Liang et al., 2021; Su et al., 2021). The main differences can be summarized as follows. First, the active faults inside the Weihe rift are well developed, and most of them have experienced historical earthquakes. They are mostly active since the late Pleistocene with intense tectonic activity, while few active faults developed in other rifts' interior. Second, the Weihe rift developed multiple groups of faults with different tectonic trends, and moderate to strong earthquakes were not only distributed on boundary faults but also on those located inside the rift. The tectonic strikes of other rifts are simple and unitary, and large earthquakes only occur on basin-controlling boundary faults. Third, the topography and geomorphology of the Weihe rift is controlled by its internal active structures and can be divided into multiple faulted-blocks. The topographic differences of other rifts are mainly located at the border between the basin and mountain, controlled by the frontal main fault.

The above evidence shows that the Weihe rift has a more complex structure, and that its tectonic evolution is affected by multiple tectonic events in time and by different tectonic stress fields in space. The discovery of the Qinghe fault not only confirms the tectonic activity inside the Weihe rift, but also reveals an active intracontinental rift. Active faults in the Weihe rift play an important role in the process of absorbing and accommodating regional tectonic deformation, which is a major factor that cannot be ignored. This is of great significance for re-determining the regional seismic hazard and understanding the evolution model of continental rifts.

5 Conclusion

A geophysical profile, boreholes, and field geologic surveys all reveal that the nearly east-west Qinghe fault developed along the Qinghe river in the Sanyuan area. The Qinghe fault zone is large, within which the main fault and the secondary faults together constitute a typical Y-shaped structure. The fact that the Qinghe fault offset a late Pleistocene paleosol, and clearly cut through Holocene strata suggests that the Qinghe fault is an active Holocene fault. Using the empirical relationship between the subsurface rupture width and the magnitude, we estimate that the maximum magnitude possible is about 5.2–5.5. The discovery of the Qinghe fault further suggests that the Weihe rift has intense tectonic activity. It is of great significance for assessing regional seismic hazards and understanding the tectonic evolution of continental rifts.

Data availability statement

The raw data supporting the conclusion of this article will be made available by the authors, without undue reservation.

Author contributions

WL and XF designed the project. WL and XF performed the fieldwork. WL analysed all the data and wrote the first draft. All authors discussed the results, provided feedback and commented on the manuscript.

Funding

This project has been supported by the National Natural Science Foundation of China (41802226; 42202255) and the National Natural Science Foundation of China (U1939201).

References

- Chen, Y., Tong, G. B., Cao, J. D., Li, Z. H., Jia, Y. K., Xu, J. M., et al. (1999). Tectonic climate response in the geomorphology of the Weihe river valley around Baoji, Shanxi province. *J. Geomechanics* 5, 51–58.
- Cheng, Y. L., He, C. Q., Rao, G., Yan, B., Lin, A. M., Hu, J. M., et al. (2018). Geomorphological and structural characterization of the southern Weihe graben, central China: Implications for fault segmentation. *Tectonophysics* 722, 11–24.
- Deng, Q. D., Cheng, S. P., Min, W., Yang, G. Z., and Ren, D. W. (1999). Discussion on Cenozoic tectonics and dynamics of Ordos block. *J. Geomechanics* 5, 13–21.
- Deng, Q. D., and Liao, Y. H. (1996). Paleoseismology along the range-front fault of Helan Mountains, north central China. *J. Geophys. Res.* 101, 5873–5893. doi:10.1029/95jb01814
- Deng, Q. D., Sung, F. M., Zhu, S. L., Li, M. L., Wang, T. L., Zhang, W. Q., et al. (1984). Active faulting and tectonics of the Ningxia-hui autonomous region, China. *J. Geophys. Res.* 89, 4427–4445. doi:10.1029/jb089i06p04427
- Deng, Q. D., Zhang, P. Z., Ran, Y. K., Min, W., Yang, X. P., and Chu, Q. Z. (2003). Basic characteristics of active tectonics of China. *Sci. China Ser. d-earth Sci.* 46, 357–372.
- Ding, Z. L., and Liu, D. S. (1989). Progresses of Loess research in China (part 1): Loess stratigraphy. *Quat. Sci.* 1, 24–35.
- Feng, X. J., Li, X. N., Ren, J., Shi, Y. Q., Dai, W. Q., Wang, F. Y., et al. (2008). The deep, middle, shallow and near surface display of the Weihe fault. *Seismol. Geol.* 30, 264–272.
- Han, J., Fyfe, W. S., Longstaffe, F. J., Palmer, H., Yan, F., and Mai, X. (1997). Pliocene-Pleistocene climatic change recorded in fluvio-lacustrine sediments in Central China. *Palaeogeogr. Palaeoclimatol. Palaeoecol.* 135, 27–39. doi:10.1016/s0031-0182(97)00019-9
- Hao, M., Wang, Q. L., Cui, D. X., Liu, L. W., and Zhou, L. (2016). Present-day crustal vertical motion around the Ordos block constrained by precise leveling and GPS data. *Surv. Geophys.* 37, 923–936. doi:10.1007/s10712-016-9375-1
- Hao, M., Wang, Q. L., Zhang, P. Z., Li, Z. J., Li, Y. H., and Zhuang, W. Q. (2021). Frame wobbling causing crustal deformation around the Ordos block. *Geophys. Res. Lett.* 48, e2020GL091008. doi:10.1029/2020GL091008
- He, C. Q., Yang, C. J., Rao, G., Yuan, X. P., Roda-Boluda, D. C., Cheng, Y. L., et al. (2020). Seismic assessment of the Weihe Graben, central China: Insights from geomorphological analyses and ¹⁰Be-derived catchment denudation rates. *Geomorphology* 359, 107151. doi:10.1016/j.geomorph.2020.107151
- Lei, Q. Y., Chai, Z. Z., Meng, G. H., Du, P., Wang, Y., Xie, X. F., et al. (2008). Composite drilling section exploration of Yinchuan buried fault. *Seismol. Geol.* 30, 254–263.
- Lei, X. Y., Ju, H. J., and Yue, L. P. (1992). Loess-Paleosol sequence at terrace of Bahe river and its significance of age. *J. Northwest Univ. Sci.* 22, 219–226.
- Lei, X. Y., and Yue, L. P. (1997). The characteristics of the late Pleistocene Loess-Paleosol sequence and their records of paleoenvironmental changes in Guanzhong, Shanxi. *Geol. Rev.* 43, 555–560.
- Li, X. N., Feng, X. J., Dai, W. Q., Shi, Y. Q., Ren, J., Li, J., et al. (2008). Activity of the lintong-chang'an fault in loess tablelands since late Pleistocene. *Seismol. Geol.* 30, 454–463.
- Liang, K., He, Z. T., Ma, B. Q., Tian, Q. J., and Liu, S. (2021). Joint-rupture pattern and newly generated structure of fault intersections on the northern margin of the Linhe Basin, northwestern Ordos Block, China. *Tectonics* 40, e2021TC006845. doi:10.1029/2021tc006845
- Liu, D. S., and Ding, Z. L. (1990). Progresses of loess research in China (part 2): Paleoclimatology and global change. *Quat. Sci.* 1, 1–9.

Conflict of interest

The authors declare that the research was conducted in the absence of any commercial or financial relationships that could be construed as a potential conflict of interest.

Publisher's note

All claims expressed in this article are solely those of the authors and do not necessarily represent those of their affiliated organizations, or those of the publisher, the editors and the reviewers. Any product that may be evaluated in this article, or claim that may be made by its manufacturer, is not guaranteed or endorsed by the publisher.

- Liu-Zeng, J., Wang, P., Zhang, Z. H., Li, Z. G., Cao, Z. Z., Zhang, J. Y., et al. (2017). Liquefaction in Western Sichuan basin during the 2008 Mw 7.9 Wenchuan earthquake, China. *Tectonophysics* 694, 214–238. doi:10.1016/j.tecto.2016.11.001
- Ma, J., Feng, X. J., Li, G. Y., Li, X. N., and Shi, Y. Q. (2019). Textual research of 1568 M7 Gaoling earthquake in Shanxi and analysis of its seismogenic structure. *Seismol. Geol.* 41, 178–188.
- McCalpin, J. P. (2009). *Paleoseismology*. San Diego, CA: Academic Press.
- Middleton, T. A., Elliott, J. R., Rhodes, E. J., Sherlock, S., Walker, R. T., Wang, W. T., et al. (2017). Extension rates across the northern Shanxi Grabens, China, from Quaternary geology, seismicity and geodesy. *Geophys. J. Int.* 209, ggx031–558. doi:10.1093/gji/ggx031
- Middleton, T. A., Walker, R. T., Parsons, B., Lei, Q., Zhou, Y., and Ren, Z. (2016). A major, intraplate, normal-faulting earthquake: The 1739 Yinchuan event in northern China. *J. Geophys. Res. Solid Earth* 121, 293–320. doi:10.1002/2015jb012355
- Molnar, P., and Tapponnier, P. (1975). Cenozoic Tectonics of Asia: Effects of a Continental Collision: Features of recent continental tectonics in Asia can be interpreted as results of the India-Eurasia collision. *Science* 189, 419–426. doi:10.1126/science.189.4201.419
- Qu, W., Lu, Z., Zhang, Q., Li, Z. H., Peng, J. B., Wang, Q. L., et al. (2014). Kinematic model of crustal deformation of Fenwei basin, China based on GPS observations. *J. Geodyn.* 75, 1–8. doi:10.1016/j.jog.2014.01.001
- Rao, G., Lin, A. M., Yan, B., Jia, D., and Wu, X. (2014). Tectonic activity and structural features of active intracontinental normal faults in the Weihe Graben, central China. *Tectonophysics* 638, 270–285. doi:10.1016/j.tecto.2014.08.019
- Rao, G., Lin, A. M., and Yan, B. (2015). Paleoseismic study on active normal faults in the southeastern Weihe Graben, central China. *J. Asian Earth Sci.* 114, 212–225. doi:10.1016/j.jseas.2015.04.031
- Shi, Y. Q., Feng, X. J., Chong, J., Bian, J. M., Zhang, A. L., Xu, G. C., et al. (2009). Active fault study of the Weihe fault zone near Loess-covered terrace scarp. *Seismol. Geol.* 31, 9–20.
- Shi, Y. Q., Li, J., Feng, X. J., Dai, W. Q., Ren, J., Li, X. N., et al. (2007). The study of paleoearthquake on Weihe fault zone. *Seismol. Geol.* 29, 607–616.
- State Seismological Bureau (Ssb) (1998). *Active Fault system around Ordos massif*. Beijing: Seismological Press.
- Su, P., He, H. L., Tan, X. B., Liu, Y. D., Shi, F., and Kirby, E. (2021). Initiation and evolution of the Shanxi Rift System in North China: Evidence from low-temperature thermochronology in a plate reconstruction framework. *Tectonics* 40, e2020TC006298. doi:10.1029/2020tc006298
- Sun, J. M. (2005). Long-term fluvial archives in the Fen Wei Graben, central China, and their bearing on the tectonic history of the India-Asia collision system during the Quaternary. *Quaternary Sci. Rev.* 24, 1279–1286. doi:10.1016/j.quascirev.2004.08.018
- Sun, J. M., and Xu, L. L. (2007). River terraces in the Fenwei Graben, central China, and the relation with tectonic history of the India-Asia collision system during the Quaternary. *Quat. Sci.* 27, 20–26.
- Wang, S. D., Shi, Y. Q., and Li, G. Y. (2018). Discovery and significance of the seismic sand liquefaction in eastern Xianyang, Shaanxi province. *China Earthq. Eng. J.* 40, 305–315. doi:10.3969/ji.ssn.1000-0844.2018.02.305
- Wells, D., and Coppersmith, K. (1994). New empirical relationships among magnitude, rupture length, rupture width, rupture area, and surface displacement. *Bull. Seismol. Soc. Am.* 84, 974–1002.
- Wesnowsky, S. G., Jones, C. H., and Scholz, D. Q. (1984). Historical seismicity and rates of crustal deformation along the margins of the Ordos block, north China. *Bull. Seismol. Soc. Am.* 74, 1767–1783. doi:10.1785/bssa0740051767

- Xu, Y. R., He, H. L., Deng, Q. D., Allen, M. B., Sun, H. Y., and Bi, L. S. (2018). The CE 1303 hongdong earthquake and the huoshan piedmont fault, Shanxi graben: Implications for magnitude limits of normal fault earthquakes. *J. Geophys. Res. Solid Earth* 123, 3098–3121. doi:10.1002/2017JB014928
- Yang, C. Y., Li, X. N., Feng, X. J., Zhu, L., Li, M., and Zhang, E. H. (2021). The Late Quaternary and present-day activities of the Kouzhen-Guanshan Fault on the northern boundary of Weihe graben basin. *Seismol. Geol.* 43, 504–520.
- Zhang, A. L. (1991). “The late quaternary activity characteristics and paleoseismic research on the qinling northern piemont fault zone, editorial committee of “active fault research,” in *Active Fault research* (Seismological Press).
- Zhang, P. Z., Zheng, D. W., and Yin, G. M. (2006). Discussion on late Genozoic growth and rise of northern margin of the Tibetan Plateau. *Quat. Sci.* 26, 5–13.
- Zhang, Y. Q., Mercier, J., and Vergely, P. (1998). Extension in the graben systems around the Ordos (China), and its contribution to the extrusion tectonics of south China with respect to Gobi-Mongolia. *Tectonophysics* 285, 41–75. doi:10.1016/s0040-1951(97)00170-4
- Zhang, Y. Q., Vergely, P., and Mercier, J. (1995). Active faulting in and along the Qinling Range (China) inferred from spot imagery analysis and extrusion tectonics of south China. *Tectonophysics* 243, 69–95. doi:10.1016/0040-1951(94)00192-c
- Zhao, B., Zhang, C. H., Wang, D. Z., Huang, Y., Tan, K., Du, R. L., et al. (2017). Contemporary kinematics of the Ordos block, North China and its adjacent rift systems constrained by dense GPS observations. *J. Asian Earth Sci.* 135, 257–267. doi:10.1016/j.jseas.2016.12.045